Effect of high-n and continuum eigenstates on the Stark effect of resonance lines of atoms and ions

E. Stambulchik and Y. Maron

Faculty of Physics, Weizmann Institute of Science, 76 100 Rehovot, Israel

(Received 9 April 1997)

We investigate the Stark effect for spectral transitions between low-lying levels of atoms and ions. We find that often a strong cancellation of the shifts of the lower and upper levels occurs, resulting in a significant reduction in the shift. For accurate calculations, therefore, one has to account for the influence of high-principal-quantum-number and continuum levels. As examples, the shifts, splitting, and intensities of the components of the Li I $2s$-$2p$, Na I $3s$-$3p$, Ba II $5d$-$6p$, Ba II $6s$-$6p$, and the quadrupole Ba II $6s$-$5d$ (shifts only) transitions are calculated for electric fields up to ≈ 20 MV/cm. Comparison of the calculated shift parameters to experimental data for the Li I $2s$-$2p$, Na I $3s$-$3p$, and Ba II $6s$-$5d$ lines, available as yet only for low fields for which the effect is quadratic, showed an excellent agreement for most of these lines. [S1050-2947(97)02610-3]

PACS number(s): 32.60.+i

I. INTRODUCTION

The investigation of emission patterns of atoms under electric fields is important for the diagnostics of numerous phenomena in plasma physics. The recent advances in high voltage technology allow electric fields up to 10 MV/cm to be produced in the laboratory [1–4]. Knowledge of the level energy shifts under high fields allows the electric field distribution to be obtained from line-emission patterns, as has been done for fields $\simeq 1$ MV/cm [5], using the $4p$-$4d$ transitions in Al III, and $\simeq 10$ MV/cm [6], using the $2s$-$2p$ transitions in Li I. For the determination of the electric fields in such studies, line-shift calculations accurate to within a very few percent are required. Here, we demonstrate that the Stark shift parameters for both the ground and first excited states are often of the same order and cancel each other to a large extent. Thus an accurate calculation of the shifts of these levels requires accounting for the effects of high-lying levels including those of the continuous spectrum. The effect of high-lying levels on the electric-field-induced shift parameters can be large when both upper and lower levels of the transition are energetically separated from the other levels, i.e., not only for principal resonance lines (for example, transitions between the $5d$ and $6p$ levels in Ba II, see below). Neglecting the contribution of the high levels may thus lead to significant errors in the calculations.

II. CALCULATION PROCEDURE

We use the n, l, m_l, m_s representation. The Hamiltonian is of the form

$$H = H_0 + V_{ls} + V_{EF}, \tag{1}$$

where H_0 is the Hamiltonian due to the Coulomb interaction (H_0 is diagonal, giving the energy levels with no ls interaction), V_{ls} is the perturbation due to the ls coupling, and V_{EF} is the perturbation due to the electric field. Here,

$$V_{ls} = A_{nl} \vec{l} \cdot \vec{s}, \tag{2}$$

where A_{nl} are constants derived from atomic level data tables (e.g., [7]), and

$$V_{EF} = -eFz, \tag{3}$$

where the electric field $\vec{F}$ is assumed to be in the z direction.

The matrix elements of Eqs. (2) and (3) can be written as

$$
\begin{aligned}
\langle n' l' & m_l' m_s' | V_{ls} | n l m_l m_s \rangle \\
&= (A_{nl}/2) \delta_{nn'} \delta_{ll'} \{ \delta_{m_s, m_{s'}-1} \delta_{m_l, m_{l'}+1} \\
&\quad \times \sqrt{(l-m_l)(l+m_l+1)} \\
&\quad + \delta_{m_s, m_{s'}+1} \delta_{m_l, m_{l'}-1} \sqrt{(l+m_l)(l-m_l+1)} \\
&\quad + 2 \delta_{m_s, m_{s'}} \delta_{m_l, m_{l'}} m_s m_l \}
\end{aligned}
\tag{4}
$$

and

$$
\begin{aligned}
\langle n' l' m_{l'} m_{s'} | F_{EF} | n l m_l m_s \rangle &= -i e a_B F (-1)^{l'-m'} \\
&\quad \times \begin{pmatrix} l' & 1 & l \\ -m' & 0 & m \end{pmatrix} (n' l' \| r \| n l).
\end{aligned}
\tag{5}
$$

The absolute values of the reduced matrix elements $(n' l' \| r \| n l)$ are derived from the oscillator strengths f for absorption of the corresponding transitions:

$$(n' l' \| r \| n l) = \sqrt{\frac{3 f_{ik} R (2l+1)}{E_i - E_k}}, \tag{6}$$

where R is the Rydberg constant and E_i and E_k are the energies of the upper and lower levels, respectively. The signs of the matrix elements, which are important for the nonquadratic Stark effect, are taken from matrix elements calculated using the code due to Cowan [8], based on the Hartree-Fock method with relativistic corrections (here called "the HFR method").

In order to limit the number of levels in the Hamiltonian matrix, we identified the levels the effect of which is very close to quadratic. These levels include the discrete levels with high principal quantum numbers and the continuum levels. The effect of those levels could be replaced by the effect of a few ''effective'' levels.

Thus the Hamiltonian matrix includes the levels taken explicitly, and, in addition, it includes the effective levels $\bar{s}$, $\bar{p}$, $\bar{d}$, ... (one level for each value of the orbital momentum that can mix with either the initial or final levels of the transition under investigation), which replace all higher levels (the discrete and the continuum ones) as stated above.

After the diagonalization of the Hamiltonian, the radius-vector matrix elements, calculated in the basis of the new wave functions, give the intensities of spectral line components in the dipole approximation.

For the sake of comparison with other studies, we also give in this paper the quadratic Stark effect parameters γ, obtained in our calculations by taking the low-field limit through the relation

$$\Delta E = \gamma F^2. \quad (7)$$

III. THE EFFECT OF THE HIGH LEVELS

As said above, we identified the discrete and the continuum levels that are high enough to cause an almost purely quadratic Stark shift of the levels concerned for the electric field range addressed. These levels are replaced by the effective levels $\bar{\alpha}$. The oscillator strength $f_{i\bar{\alpha}}$ between a low-lying level i with an energy E_i and the effective level $\bar{\alpha}$ with an energy $E_{\bar{\alpha}}$ can be calculated using the following identity:

$$\frac{f_{i\bar{\alpha}}}{(E_i - E_{\bar{\alpha}})^2} = \sum_k \frac{f_{ik}}{(E_i - E_k)^2} + \int dE \frac{df/dE}{(E_i - E)^2}, \quad (8)$$

where the summation and integration, respectively, are carried out over the high discrete levels and the continuum levels that are replaced by the effective levels.

The transition probability between the level i and the discrete levels that are close to the continuum region is proportional to the energy level density, i.e., to $1/n^3$. Therefore, for high n, f_{ik} can be assumed to obey

$$f_{ik} = \frac{\lambda_i}{n^3}. \quad (9)$$

The coefficients λ_i are obtained from the HFR-code calculations for n varying within an appropriate range of high values and taking limits of the series. The uncertainties in the coefficients due to this procedure cause no significant error in the calculation of the total quadratic Stark effect since the contribution of the high-n discrete levels is small compared to that of the continuum levels. This is shown in Table I for Li I, where the quadratic constants γ due to the high-n discrete levels and due to the continuum levels are given separately.

The values of df/dE for the continuous-spectrum wave functions are calculated by the HFR code. The energies of

TABLE I. Values of γ [$\text{cm}^{-1}/(\text{MV/cm})^2$] for the Li I $2s$ and $2p$ levels due to the $n > 10$ and the continuum levels.

Level	γ due to the $n > 10$ levels	γ due to the continuum levels
$2s_{1/2,1/2}$	$-1.58(-4)$	$-4.88(-3)$
$2p_{1/2,1/2}$	$-4.49(-3)$	$-3.01(-2)$
$2p_{3/2,1/2}$	$-5.22(-3)$	$-3.54(-2)$
$2p_{3/2,3/2}$	$-3.75(-3)$	$-2.49(-2)$

the effective levels $E_{\bar{\alpha}}$ can be chosen arbitrarily, provided they are chosen to be high enough to satisfy the assumption of a pure quadratic Stark effect.

The energy levels $E_{\bar{\alpha}}$ and the oscillator strengths $f_{i\bar{\alpha}}$ thus obtained are used in the Hamiltonian matrix, in order to replace all high-n discrete levels and continuum levels.

IV. AVOIDED CROSSINGS

In calculating the Stark effect for strong electric fields, the problem of avoided crossings has to be treated properly. For high fields the Rydberg levels can be shifted close to the levels under investigation. This can strongly affect the shifts of the lower levels, if they mix with the Rydberg levels. As a very simplified example, let us consider the following effective two-level Hamiltonian:

$$H = H_0 + V,$$

with

$$H_0 = \begin{pmatrix} E_{\text{Ry}} & 0 \\ 0 & E_0 \end{pmatrix} \quad \text{and} \quad V = \begin{pmatrix} -\alpha F & \beta F \\ \beta F & \bar{\gamma} F^2 \end{pmatrix}.$$

Here, E_0 and E_{Ry} are the unperturbed energies of the lower level and the Rydberg level, respectively, α gives the linear shift of the Rydberg state, β gives the mixing between the two levels, and $\bar{\gamma}$ is the coefficient of the quadratic Stark effect for the lower level due to the interaction with the rest of the atomic levels (this is what we mean by ''effective two-level Hamiltonian''). For α, β, and $\bar{\gamma}$ satisfying

$$\frac{\beta}{\alpha} \ll 1; \quad \frac{\bar{\gamma}(E_{\text{Ry}} - E_0)}{\alpha^2} \ll 1,$$

the distance between the levels approaches its minimal value of $\simeq 2(\beta/\alpha)(E_{\text{Ry}} - E_0)$ at the electric field $F_0 \simeq (E_{\text{Ry}} - E_0)/\alpha$. Near this point the shifts and intensities vary sharply as a function of the electric field. However, one has to consider the Rydberg-level field ionization at electric fields lower than F_0. If this happens, the Rydberg state joins the continuum, making this picture unrealistic. In the calculations, it is possible to avoid this problem by preventing the Rydberg levels from splitting linearly for fields larger than the field-ionization threshold. This is made in our calculations by forcing the radius-vector matrix elements between different sublevels with the same principal quantum number to be 0 at electric fields exceeding the ionization threshold of these levels. These thresholds were determined by the semiclassical method ([12], and references therein).

TABLE II. Values of the total γ [cm^{-1}/(MV/cm)^2] and of γ only due to the high-n and the continuum levels for the Li I 2s and 2p levels.

Level	Total γ	γ due to the high-n and the continuum levels
$2s_{1/2,1/2}$	-0.680	$-5.04(-3)$
$2p_{1/2,1/2}$	-0.526	$-3.46(-2)$
$2p_{3/2,1/2}$	-0.518	$-4.05(-2)$
$2p_{3/2,3/2}$	-0.533	$-2.87(-2)$

V. RESULTS

A. Li I transitions

The oscillator strengths of the Li I 2s-2p and 2p-3s transitions are taken from Ref. [9], of the 2p-3d from Ref. [10], and all others between levels up to $n=10$ are taken from Ref. [11].

The quadratic-effect constants γ for the levels and for the transitions are given in Tables II and III, respectively. In both tables, the left columns give the total values of γ and the right columns give the values due to the high-n discrete levels and the continuum levels. One can see that the contributions of these levels to the shifts of the upper or lower levels of the 2s-2p transition are less than 8%. However, due to the strong cancellation of the 2s and 2p shifts, the contributions of the high levels to the shifts of the transition components reach $\simeq$20% (in fact, they only reach $\simeq$20%, in spite of the strong cancellation, since the cancellation also occurs for the high-level contributions, as can be inferred from Table II).

The calculated Stark shifts for the 2s-2p transitions of Li I as a function of the electric field are shown by the solid lines in Fig. 1. Intensities of the different components of the line as a function of the electric field are given by the solid lines in Fig. 2. In the figures, note the crossing of the energy levels at a field $\simeq$8.5 MV/cm, which breaks the monotonous behavior of the component intensities. The crossing of the energy levels is caused by the deviation of the Stark effect from the quadratic one.

To illustrate the importance of the nonquadratic Stark effect we also calculate the shift and intensities assuming a pure quadratic effect for all levels. This was implemented by substituting *all* levels, except for the 2p and 2s levels, by three effective levels that give the quadratic Stark shift con-

TABLE III. Values of the total γ [cm^{-1}/(MV/cm)^2] and of γ only due to the high-n and the continuum levels for the Li I 2s-2p transitions.

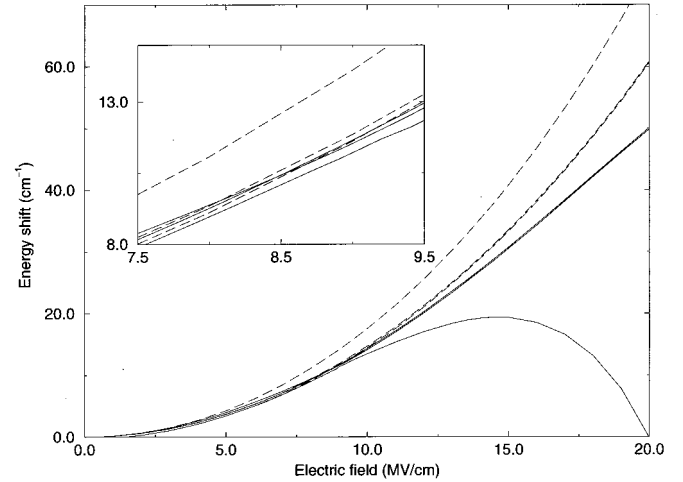| Transition	Total γ	γ due to the high-n and the continuum levels
$2s_{1/2,1/2}$-$2p_{1/2,1/2}$	0.154	$-2.96(-2)$
$2s_{1/2,1/2}$-$2p_{3/2,1/2}$	0.162	$-3.55(-2)$
$2s_{1/2,1/2}$-$2p_{3/2,3/2}$	0.147	$-2.37(-2)$

FIG. 1. The Stark shifts of the Li I 2s-2p line components as a function of the electric field (solid lines). The quadratic-effect shifts are shown by the dashed lines. The region of the energy level crossing is given in the inset.

stants γ, using the method described in Sec. III. The results are shown by the dashed lines in Figs. 1 and 2 (the dashed curves differ from pure parabolas with constants γ due to the ls interaction). The significant deviations of the intensities at fields above 5 MV/cm and of the shifts at fields above 10 MV/cm from the quadratic behavior are seen.

The present calculations of the quadratic effect can be compared to the calculations given in Ref. [13]. The difference is about 100% for the shift constants of the transition components. It is possible that in Ref. [13] the contribution of the continuum levels was not taken into account. However, based on the present calculations, this neglect can only account for a discrepancy of $\simeq$20% between the two calculations.

There are other theoretical calculations of the Li I Stark parameters performed using different techniques. In Ref. [14] only presented is the quadratic-effect constant for the Li I $D1(2s_{1/2}$-$2p_{1/2})$ line, which coincides with ours to
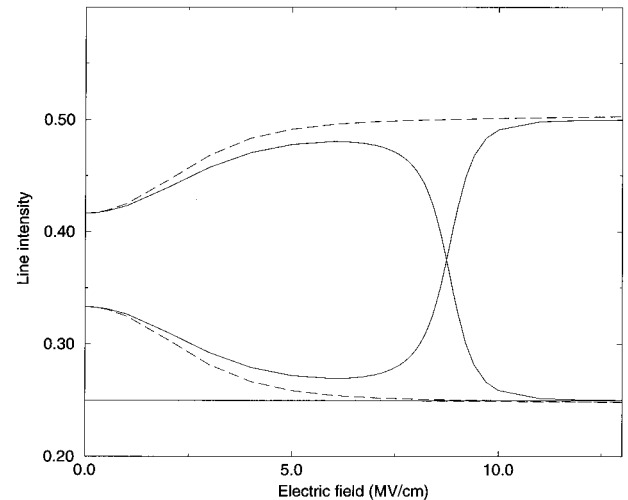

FIG. 2. Intensities of the Li I 2s-2p line components as a function of the electric field (solid lines). Here, the observation direction is perpendicular to the electric field. The quadratic-effect intensities are shown by the dashed lines.
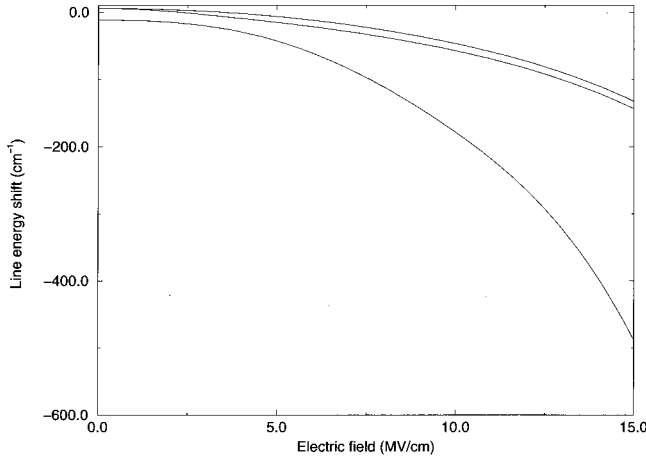
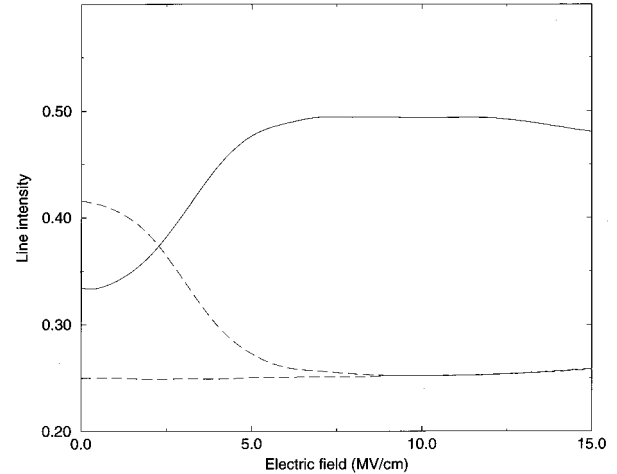FIG. 3. The Stark shifts of the Na I $3s$-$3p$ line components as a function of the electric field.

FIG. 4. Intensities of the Na I $3s$-$3p$ line components as a function of the electric field. The observation direction is perpendicular to the electric field. The solid line corresponds to the $3s_{1/2}$-$3p_{1/2}$ component and the dashed lines correspond to the $3s_{1/2}$-$3p_{3/2}$ components.

within 0.5%. It is of special interest, however, to compare our results to calculations for high fields. In this respect, the only study known to us is that given in Ref. [15]. For an electric field of 10 MV/cm the differences are $\simeq$25% and 15% for the $2s0$-$2p0$ and $2s0$-$2p\pm1$ components of the line. For an electric field of 15 MV/cm the differences are $\simeq$35% and 5%, respectively. For fields much lower than 10 MV/cm, the comparison between the results of Ref. [15] and our study is not possible, since in Ref. [15] the fine coupling (that is important for such fields) was neglected.

Due to the strong cancellation of the redshifts and blueshifts, the uncertainties in the oscillator strengths cause large errors in the total shift. For example, an error of 1% in the oscillator strength of the $2s$-$2p$ transition produces an error of 6% in the total shift. However, the $2s$-$2p$, $2p$-$3s$, and $2p$-$3d$ oscillator strengths were calculated with a high accuracy. The uncertainties for the first two are believed to be $<$0.1%, and for the third one better than 0.5% [9,10]. Therefore these uncertainties are expected to affect the accuracy in our calculations by less than 1%. The other important transitions are the $2p$-nd transitions that contribute about 75% of the total shift. The oscillator strengths of these transitions differ from the hydrogenic ones by less than 10%. We believe, therefore, that their calculated values are accurate to within a few percent. Thus, accounting for the uncertainties of all oscillator strengths that affect the $2s$-$2p$ line shifts, we believe that the uncertainty in our line-shift calculations is $\simeq$5%.

However, in spite of the uncertainties in the oscillator strengths, the present calculations appear to be rather accurate for low fields. We compare them to experimental data for fields up to 400 kV/cm obtained with an accuracy of $\simeq$0.5% [16] and $\simeq$0.1% [17]. For these fields the Stark shift is quadratic. Our quadratic constants for all components of the $2s$-$2p$ transition were found to agree to within $<$1% with the experimental ones. This good agreement could result either from a coincidental cancellation of the errors in the oscillator strengths or from accuracies in the oscillator strength calculations that are better than quoted above.

B. Na I transitions

Here, levels with $n \leqslant 10$ were included explicitly. For the levels with principal quantum number up to 6 we used the

oscillator strengths given in Ref. [18], and for the other levels we used the calculations given in Ref. [11].

The calculated Stark shifts for the $3s$-$3p$ transitions in Na I are shown as a function of the electric field in Fig. 3, and the intensities of the different components of the line are given in Fig. 4. The Stark effect for this Na I line deviates from a quadratic behavior (not shown in Fig. 3) for fields lower than for Li I: the deviation is about 10% at 2 MV/cm and $\simeq$100% at 10 MV/cm.

Calculated values for the quadratic effect for the $3s$ and $3p$ levels are given in Table IV and the values of the quadratic Stark shift parameters for the Na I $3s$-$3p$ line components are given in Table V. Comparison of the quadratic-shift parameters given in Table V with precise measurements [19] for fields up to 150 kV/cm shows an agreement to within 1%. It is also seen in Table V that the contribution of the high-n and continuum levels to the total line shifts is less than 2%, i.e., the relative contribution of these levels is lower than for Li I.

C. Ba II transitions

The oscillator strengths between levels with the principal quantum number up to 12, used to calculate the Stark effect

TABLE IV. Values of the total γ [cm^{-1}/(MV/cm)^2] and of γ only due to the high-n and the continuum levels for the Na I $3s$ and $3p$ levels.

Level	Total γ	γ due to the high-n and the continuum levels
$3s_{1/2,1/2}$	-0.671	$-3.1(-4)$
$3p_{1/2,1/2}$	-1.498	$-2.6(-2)$
$3p_{3/2,1/2}$	-1.865	$-3.1(-2)$
$3p_{3/2,3/2}$	-1.136	$-2.0(-2)$

TABLE V. Values of the total γ [cm^{-1}/(MV/cm)^2] and of γ only due to the high-n and the continuum levels for the Na I $3s$-$3p$ transitions.

Transition	Total γ	γ due to the high-n and the continuum levels
$3s_{1/2,1/2}$- $3p_{1/2,1/2}$	-0.827	$-2.6(-2)$
$3s_{1/2,1/2}$- $3p_{3/2,1/2}$	-1.194	$-3.1(-2)$
$3s_{1/2,1/2}$- $3p_{3/2,3/2}$	-0.465	$-2.0(-2)$

of Ba II lines, were taken from [11] except those for the $6s$-$6p$ and $5d$-$6p$ transitions for which the recently measured values [20] were used.

Figure 5 presents the Stark shifts of the Ba II $6s$-$6p$ transitions. We do not show intensities of the Ba II $6s$-$6p$ transition components because they do not deviate from their zero-field values by more than 2% even for electric field of 20 MV/cm. Figures 6–8 and 9, respectively, give the Stark shifts and intensities of the Ba II 5d–6p transitions. The enlarged regions, given in insets in Figs. 6 and 7, show changes in the sign of the shifts of the $5d_{3/2,3/2}$-$6p_{1/2,1/2}$ and the $5d_{3/2,3/2}$-$6p_{3/2,1/2}$ components, respectively.

Calculated values for the quadratic effect for the levels are given in Table VI. It is seen that the contribution of the high-n and continuum levels to γ may reach about 10%. For transitions for which the Stark shift is particularly small (due to cancellation), the effect of these high levels can be very significant. Thus, for the $5d_{3/2,3/2}$-$l6p_{1/2,1/2}$ and the $5d_{3/2,3/2}$-$6p_{3/2,1/2}$ transitions, where the Stark shift is calculated to be close to zero (see below), the contribution of the high levels to the Stark shift exceeds 100%.

The uncertainty in the oscillator strengths most important for the calculations, i.e., of the $6s$-$6p$ and $5d$-$6p$ transitions, is ≈ 4%, see [20]. Together with the uncertainty of $\simeq 10$% of the rest of the oscillator strengths, this leads to an uncertainty of $\simeq 2(-2)$ cm^{-1}/(MV/cm)^2 for all levels mentioned above. While this causes an uncertainty of about 10% in the shifts of a few components of these transitions, it does cause a large relative uncertainty for small line shifts (where can-
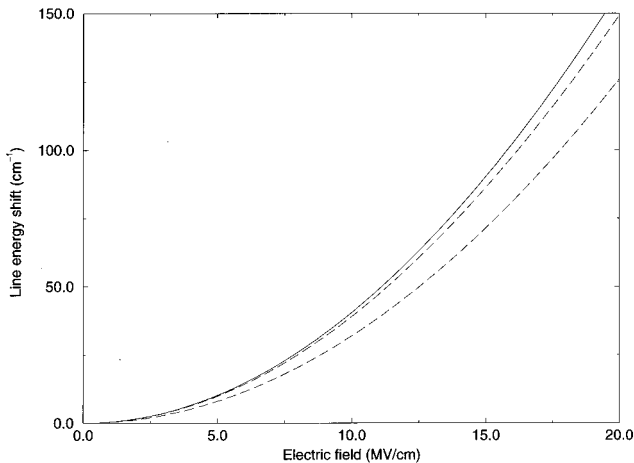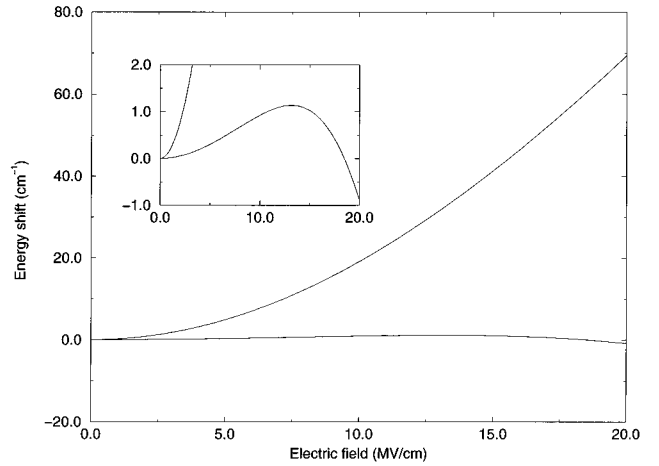

FIG. 6. The Stark shifts of the Ba II $5d_{3/2}$-$6p_{1/2}$ line components as a function of the electric field. The enlarged region in the inset shows the change in sign of the $5d_{3/2,3/2}$-$6p_{1/2,1/2}$ component.

cellation occurs). For example, it even causes an uncertainty in the sign of the $5d_{3/2,3/2}$-$6p_{1/2,1/2}$ and $5d_{3/2,3/2}$-$6p_{3/2,1/2}$ shifts. For the rest of the Ba II $6s$-$6p$ and $5d$-$6p$ line components, the Stark effect is almost quadratic up to 20 MV/cm, the deviations from the quadratic dependence do not exceed 10% for that field. Table VII shows calculated values of the quadratic Stark shift parameters for all Ba II $6s$-$6p$ and $5d$-$6p$ line components.

Our calculations allow us to obtain the quadratic Stark shift parameters for the quadrupole Ba II $6s_{1/2}$-$5d_{5/2}$ transition. These are given in Table VIII together with recently measured Stark shift parameters for this transition [21]. It is seen that the present calculations give results that coincide with the measured values to within the experimental errors (± 10%).

VI. THE EFFECT OF MAGNETIC FIELD

In the calculations described above, the effect of the magnetic field on the line splitting can be easily accounted for.
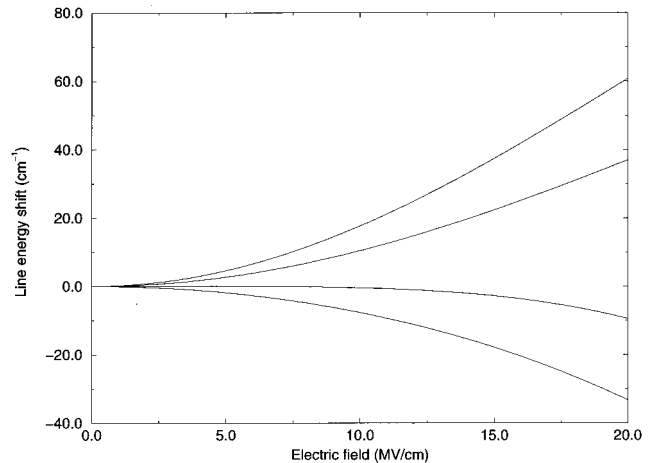

FIG. 5. The Stark shift of the Ba II $6s_{1/2}$-$6p_{1/2}$ line (solid line) and shifts of the Ba II $6s_{1/2}$-$6p_{3/2}$ line components (dashed lines) as a function of the electric field.

FIG. 7. The Stark shifts of the Ba II $5d_{3/2}$-$6p_{3/2}$ line components as a function of the electric field. The enlarged region in the inset shows the change in sign of the shift of the $5d_{3/2,3/2}$-$6p_{3/2,1/2}$ component.
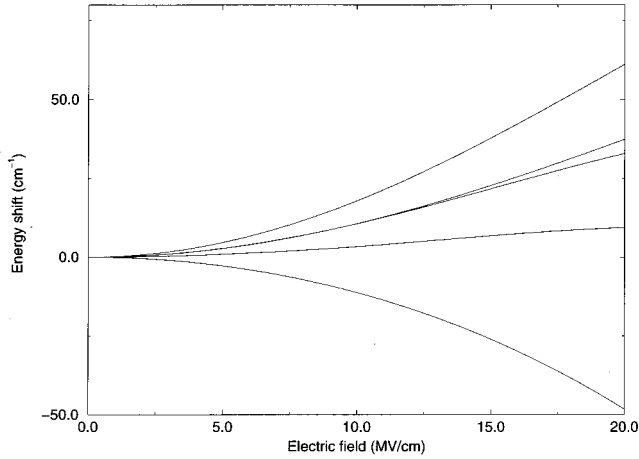
FIG. 8. The Stark shifts of the Ba II $5d_{5/2}$-$6p_{3/2}$ line components as a function of the electric field.

To this end, we modify the formula (1) to

$$H = H_0 + V_{ls} + V_{EF} + V_{MF}, \tag{10}$$

where V_{MF} is the perturbation due to the magnetic field $\vec{B}$ and can be expressed as

$$V_{MF} = \mu \vec{B} \cdot (\vec{l} + g_e \vec{s}). \tag{11}$$

Here, μ is the Bohr magneton and g_e is the g factor of the electron.

The matrix elements of Eq. (11) can be written as

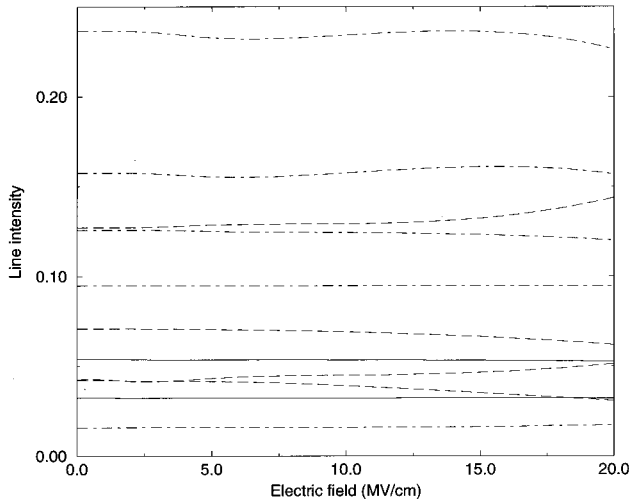FIG. 9. Intensities of the Ba II $5d$-$6p$ line components as a function of the electric field. The observation direction is perpendicular to the electric field. The solid, dashed, and dot-dashed lines correspond to the $5d_{3/2}$-$6p_{1/2}$ components, the $5d_{3/2}$-$6p_{3/2}$ components, and the $5d_{5/2}$-$6p_{3/2}$ components, respectively.

TABLE VI. Values of the total γ [cm^{-1}/(MV/cm)^2] and of γ only due to the high-n and the continuum levels for the Ba II $6s$, $5d$, and $6p$ levels.

Level	Total γ	γ due to the high-n and the continuum levels
$6s_{1/2,1/2}$	-0.457	$-7.0(-5)$
$5d_{3/2,1/2}$	-0.244	$-7.1(-3)$
$5d_{3/2,3/2}$	-0.060	$-4.3(-3)$
$5d_{5/2,1/2}$	-0.246	$-7.3(-3)$
$5d_{5/2,3/2}$	-0.173	$-6.2(-3)$
$5d_{5/2,5/2}$	-0.025	$-3.8(-3)$
$6p_{1/2,1/2}$	-0.049	$-6.4(-3)$
$6p_{3/2,1/2}$	-0.061	$-8.5(-3)$
$6p_{3/2,3/2}$	-0.137	$-4.6(-3)$

$$\langle n'l'm_{l'}m_{s'} | V_{MF} | nlm_l m_s \rangle$$
$$= (\mu/2)\delta_{nn'}\delta_{ll'}\{(B_x - iB_y)$$
$$\times [\delta_{m_{l'},m_l+1}\sqrt{(l-m_l)(l+m_l+1)} + \delta_{m_{s'},m_s+1}g_e]$$
$$+ (B_x + iB_y)[\delta_{m_{l'},m_l-1}\sqrt{(l+m_l)(l-m_l+1)}$$
$$+ \delta_{m_{s'},m_s-1}g_e] + 2B_z(\delta_{m_l,m_{l'}}m_l + \delta_{m_s,m_{s'}}g_e m_s)\}. \tag{12}$$

This modification allows one to calculate the emission pattern of the spectral lines under the combined effects of electric and magnetic fields.

VII. SUMMARY

The importance of the effect of the high-principal-quantum-number and continuum levels on the shift and splitting of spectral patterns of transitions between low-lying levels of atoms and ions is shown. This becomes important due

TABLE VII. Values of the total γ [cm^{-1}/(MV/cm)^2] and of γ only due to the high-n and the continuum levels for the Ba II $6s$-$6p$ and $5d$-$6p$ transitions.

Transition	Total γ	γ due to the high-n and the continuum levels
$6s_{1/2,1/2}$-$6p_{1/2,1/2}$	0.408	$-6.3(-3)$
$6s_{1/2,1/2}$-$6p_{3/2,1/2}$	0.396	$-8.4(-3)$
$6s_{1/2,1/2}$-$6p_{3/2,3/2}$	0.320	$-4.5(-3)$
$5d_{3/2,1/2}$-$6p_{1/2,1/2}$	0.195	$7.0(-4)$
$5d_{3/2,3/2}$-$6p_{1/2,1/2}$	0.011	$-2.1(-3)$
$5d_{3/2,1/2}$-$6p_{3/2,1/2}$	0.183	$-1.4(-3)$
$5d_{3/2,3/2}$-$6p_{3/2,1/2}$	-0.001	$-4.2(-3)$
$5d_{3/2,1/2}$-$6p_{3/2,3/2}$	0.107	$2.5(-3)$
$5d_{3/2,3/2}$-$6p_{3/2,3/2}$	-0.077	$-3.0(-4)$
$5d_{5/2,1/2}$-$6p_{3/2,1/2}$	0.185	$-1.2(-3)$
$5d_{5/2,3/2}$-$6p_{3/2,1/2}$	0.112	$-2.3(-3)$
$5d_{5/2,1/2}$-$6p_{3/2,3/2}$	0.109	$2.7(-3)$
$5d_{5/2,3/2}$-$6p_{3/2,3/2}$	0.036	$1.6(-3)$
$5d_{5/2,5/2}$-$6p_{3/2,3/2}$	-0.112	$-8.0(-4)$

TABLE VIII. Values of γ [cm^{-1}/(MV/cm)^2] for the Ba II $6s_{5/2}$-$5d_{1/2}$ transitions.

Transition	Present calculations	Experiment
$6s_{1/2,1/2}$-$5d_{5/2,1/2}$	0.211	0.20 ± 0.02
$6s_{1/2,1/2}$-$5d_{5/2,3/2}$	0.284	0.25 ± 0.03
$6s_{1/2,1/2}$-$5d_{5/2,5/2}$	0.432	0.39 ± 0.04

to a strong cancellation of the shifts of the lower and upper levels, resulting in a significant reduction in the line shift that consequently increases the influence of the high levels. The shifts and intensities of the Stark components of a few spectral lines were calculated for electric fields up to $\approx$20 MV/cm. The calculated shift parameters are in very good agreement with experimental measurements, as yet only available for low fields.

[1] J. P. VanDevender and P. L. Cook, Science **232**, 801 (1986).
[2] B. P. Aduev and V. G. Shpak, Instrum. Exp. Tech. **33**, Iss. 2, 280 (1990).
[3] I. Smith, in *Proceedings of the 8th International Pulsed Power Conference, San Diego,* edited by R. White and K. Prestwitch (Institute of Electrical and Electronics Engineers, New York, 1991), pp. 15–22.
[4] G. A. Mesyats *et al.*, Sov. Phys. J. **12**, 688 (1969).
[5] Y. Maron *et al.*, Phys. Rev. Lett. **57**, 699 (1986).
[6] J. Bailey *et al.*, Phys. Rev. Lett. **74**, 1771 (1995).
[7] C. E. Moore, *Atomic Energy Levels*, Natl. Bur. Stand. (U. S.) Natl. Bur. Stand. Ref. Data Ser. 35 (U. S. GPO, Washington, DC, 1971), Vol. I.
[8] R. D. Cowan, *The Theory of Atomic Structure and Spectra* (University of California Press, Berkeley, 1981).
[9] S. A. Blundell *et al.*, Phys. Rev. A **40**, 2233 (1989).
[10] J. Pipin and D. M. Bishop, Phys. Rev. A **45**, 2736 (1992).
[11] A. Lindgård and S. E. Nielsen, At. Data Nucl. Data Tables **19**, 553 (1977).
[12] H. A. Bethe and E. E. Salpeter, *Quantum Mechanics of One- and Two-Electron Atoms* (Plenum/Rosetta Edition, New York, 1977).
[13] K. Murakawa and M. Yamamoto, J. Phys. Soc. Jpn. **20**, 1057 (1965).
[14] J. Pipin and D. M. Bishop, Phys. Rev. A **47**, 4571 (1993).
[15] C. A. Nicolaides and S. I. Themelis, Phys. Rev. A **47**, 3122 (1993).
[16] L. Windholz *et al.*, Phys. Rev. A **46**, 5812 (1992).
[17] L. R. Hunter *et al.*, Phys. Rev. A **44**, 6140 (1991).
[18] C. Laughlin, Phys. Scr. **45**, 235 (1992).
[19] L. Windholz and M. Musso, Phys. Rev. A **39**, 2472 (1989).
[20] M. D. Davidson *et al.*, Astron. Astrophys. **255**, 457 (1992).
[21] N. Yu *et al.*, Phys. Rev. A **50**, 2738 (1994).